# Coexistence of Light and Heavy Carriers Associated with Superconductivity and Antiferromagnetism in $CeNi_{0.8}Bi_2$ with a Bi Square Net

Hiroshi Mizoguchi,[1] Satoru Matsuishi,[2] Masahiro Hirano,[1] Makoto Tachibana,[3] Eiji Takayama-Muromachi,[3] Hitoshi Kawaji,[2] and Hideo Hosono[1,2,*]

[1]*Frontier Research Center, Tokyo Institute of Technology, 4259 Nagatsuta, Midori-ku, Yokohama 226-8503, Japan*
[2]*Materials and Structures Laboratory, Tokyo Institute of Technology, 4259 Nagatsuta, Midori-ku, Yokohama 226-8503, Japan*
[3]*National Institute for Materials Science, 1-1 Namiki, Tsukuba, Ibaraki 305-0044, Japan*

(Received 21 September 2010; published 2 February 2011)

We found that the ZrCuSiAs-type crystal $CeNi_{0.8}Bi_2$ with a layered structure composed of alternate stacking of $[CeNi_xBi(1)]^{\delta+}$ and $Bi(2)^{\delta-}$ exhibits a superconductive transition at ~4 K. The conductivities, magnetic susceptibilities, and heat capacities measurements indicate the presence of two types of carriers with notable different masses, i.e., a light electron responsible for superconductivity and a heavy electron interacting with the Ce $4f$ electron. This observation suggests that $6p$ electrons of Bi(2) forming the square net and electrons in $CeNi_xBi(1)$ layers primarily correspond to the light and heavy electrons, respectively.

DOI: 10.1103/PhysRevLett.106.057002 PACS numbers: 74.70.Xa, 71.20.Ps

Significant attention has been paid towards ZrCuSiAs-type compounds [1–10] since the discovery of superconductivity in F-doped LaFeAsO with a transition temperature ($T_c$) of 26 K. Maintaining the basic structural unit of FeAs, several new systems, such as LiFeAs (111), $AFe_2As_2$ ($A$ = Sr and Ba) (122) and $FeSe_{1-x}$ (11) have been found to exhibit superconductivity, which coexists with an antiferromagnetic (AFM) state at low temperature. A large variety of superconductive compounds belonging to these layered crystal structures [11] provide a good platform to explore novel superconductors and to clarify the high $T_c$ mechanism. ZrCuSiAs-type compounds contain two types of anions. There are materials in which the same types of anions occupy the anionic sites. For example, $RNi_xBi_2$ ($R$ = Ce, Nd, Gd, Tb, Dy, and Y) contains two types of Bi ions: Bi(1) forms $NiBi_4$ and Bi(2) forms a Bi square net and the formal charge of the former is −3, whereas the latter has a charge of −1 [12,13]. Figure 1 shows the crystal structure of $CeNi_xBi_2$, revealed by powder neutron structure analysis [14] in comparison with LaFeAsO [1]. Ni ions (the formal valence state is +1) with a stoichiometric composition deficiency occupy tetrahedral sites and form a distorted tetrahedron with Bi(1) ions with a formal charge state of −3. Taking into consideration the ionic sizes of Ni and Ce, Bi(2) with the formal charge state of −1 occupies a narrower space, resulting in a shorter Bi(2)-Bi(2) spacing of 3.21 Å, which arises from the covalent nature of the bond (Bi $6p$-Bi $6p$ $\sigma/\pi$ bonding). This Bi array is called the "Bi(2) square net" [11,15], where the Bi $6p$ band is not fully occupied because $Bi^{-1}$ has an electronic configuration of $(6s)^2(6p)^4$. The higher valence state of the Bi(2) makes the Ce-$Bi(2)^{-1}$ distance (3.45 Å) longer than Ce-$Bi(1)^{-3}$ (3.34 Å), and the Ce ion forms tighter bonds with the more negative Bi(1) ion. The two-dimensional electronic structure of the Bi(2) square net overlaps with the $Ni_xBi(1)$ conductive layer near the Fermi level ($E_F$). In this Letter, we report that $CeNi_xBi_2$ exhibits transitions due to both superconductivity at ~4 K and AFM at ~5 K, and the light electron of Bi(2) is responsible for the superconductivity, whereas the heavy electron is responsible for the strong interaction with Ce $4f$ which yields the AFM transition.

According to Refs. [12,13], there exists distinct off-stoichiometry of Ni in this series of compounds. Thus, the optimal Ni content was determined in an effort to minimize the impurity phase identified by powder x-ray diffraction (XRD). Polycrystalline samples of $RNi_xBi_2$ ($R$ = La, Ce, Nd, and Y) were synthesized by solid-state reactions at elevated temperatures in evacuated silica ampoules. Starting materials used were La (99.9%), Ce (99.9%), Nd (99.9%), Y (99.9%), Ni (99.9%), and Bi (99.9%). Appropriate amounts of these mixtures

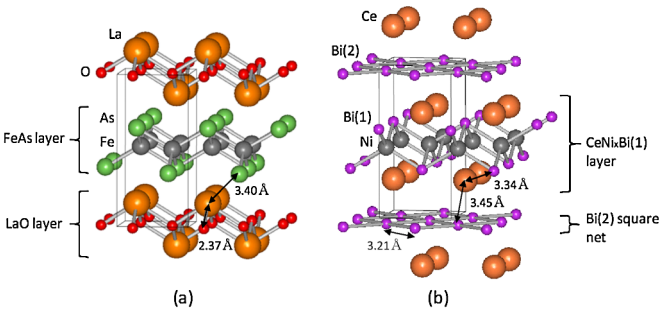


FIG. 1 (color online). Crystal structures of (a) LaFeAsO and (b) $CeNi_xBi_2$ belonging to the ZrCuSiAs type [1,14]. The valence state of each ion in (b): +3 for Ce, +1 for Ni, −3 for Bi(1), and −1 for Bi(2). Since there is a large valence difference between Bi(1) and Bi(2), the $Ce^{3+}$ that locates at sites between the two Bi layers is relaxed to the Bi(1) layers with larger negative charges, and the remaining Bi(2) forms a square net.

 

corresponding to the optimal $x$ value were heated in evacuated silica ampoule at 773 K for 10 h, followed by heat treatment at 1023 K for 20 h. The products obtained were ground and pressed into pellets and an additional heat treatment was performed in evacuated silica ampoules at 1073 K for 10 h. All the treatments of the starting materials were performed in an Ar-filled glovebox ($O_2$, $H_2O <$ 1 ppm). The crystal structure of the synthesized materials was examined by XRD) (Bruker D8 Advance TXS) using Cu $K_\alpha$ radiation with the aid of Rietveld refinement using code TOPAS3 [16]. The temperature dependence of the dc electrical resistivity ($\rho$) at 2–300 K was measured using a conventional four-probe method using Ag paste as the electrodes. Magnetization ($M$) measurements were performed with a vibrating sample magnetometer (Quantum Design). Specific heat data were obtained using a conventional thermal relaxation method using Quantum Design PPMS.

Sintered $R\mathrm{Ni}_x\mathrm{Bi}_2$ polycrystalline samples with a dark gray color and metallic luster decompose gradually into powder when exposed to an ambient atmosphere. Thus, the samples were stored in evacuated desiccators before measurements. The structure was confirmed to be ZrCuSiAs type by powder XRD measurements. For the Ce compound, inductively coupled plasma spectroscopy was employed to confirm the chemical composition, $\mathrm{CeNi}_{0.8}\mathrm{Bi}_2$, which was consistent with the result obtained by the Rietveld refinement to the XRD patterns as well as the batch composition. Table I summarizes the Ni content ($x$), lattice constants, and unit cell volume for $R\mathrm{Ni}_x\mathrm{Bi}_2$. Although the Ni content fluctuates with the $R$ ion, the unit cell volumes changed monotonically with the atomic number of the $R$ ion, according to the lanthanide contraction rule, suggesting that the Ce ion takes a +3 charge state in $\mathrm{CeNi}_{0.8}\mathrm{Bi}_2$. Figure 2(a) shows the resistivity-temperature ($\rho$-$T$) curve for $\mathrm{CeNi}_{0.8}\mathrm{Bi}_2$ under an applied magnetic field of 0 Oe. The resistivity is almost independent of $T$ above 100 K, but decreases almost linearly with $T$ at $T < 100$ K. With a further decrease in $T$, $\mathrm{CeNi}_{0.8}\mathrm{Bi}_2$ shows a $T^2$ dependence below 10 K. Although the absolute $\rho$ value varies with samples by an order of magnitude, the overall features remain unchanged. As shown in the inset of Fig. 2(a), a sharp drop in $\rho$ was observed at $T = 4.2$ K, and the resistivity vanished at 4.0 K. The $T_c$ shifts to a lower side with increasing $H$, suggesting that the $\mathrm{CeNi}_{0.8}\mathrm{Bi}_2$ undergoes a superconducting transition at 4.2 K. The magnetic susceptibilities ($\chi$) measured in zero-field cooling processes (ZFC) reached $-5.0$ emu/mol Ce [Fig. 2(b)]. This value corresponds to the volume fraction of the superconductivity phase of 96% (estimated from the $\chi$ value of perfect diamagnetism), which confirms that the bulk superconductive transition

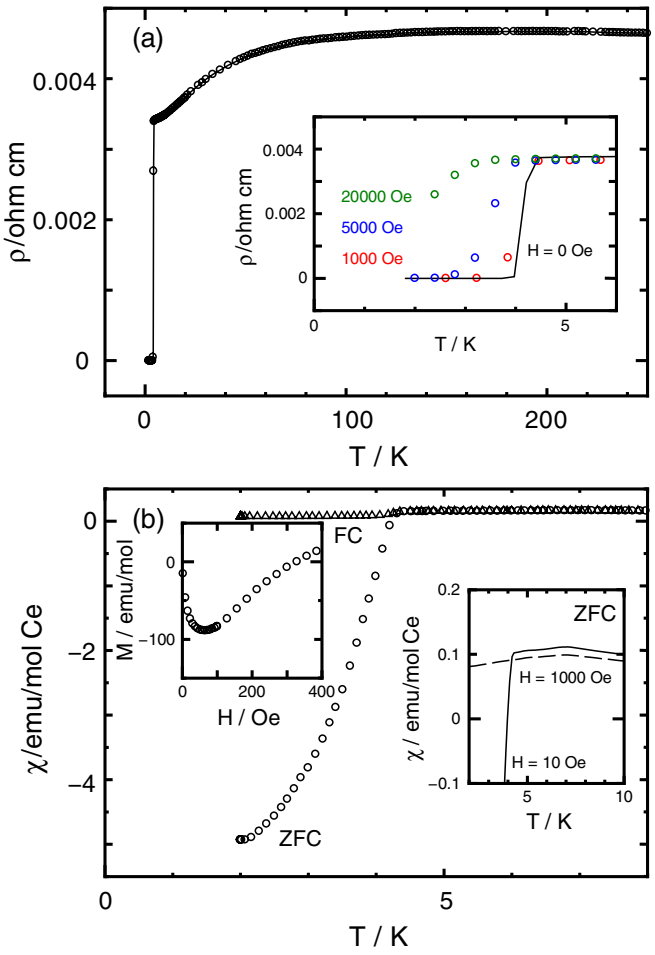


FIG. 2 (color online). (a) Temperature dependence of the electrical resistivity ($\rho$) for $\mathrm{CeNi}_{0.8}\mathrm{Bi}_2$ at 0 Oe. The inset shows the $\rho$-$T$ curves as a function of the magnetic field. (b) Temperature dependence of the magnetic susceptibility ($\chi$) under conditions of ZFC and FC at 10 Oe. The right-hand inset shows an enlargement around the transition under the condition of ZFC. Two measurement fields, 10 and 1000 Oe were used. The left-hand inset shows the field dependence of the magnetization at 2 K.

TABLE I. Lattice constants and unit cell volumes of $R\mathrm{Ni}_x\mathrm{Bi}_2$. The lattice constants were determined by LeBail fitting [17].

| R | La | Ce [14] | Nd | Gd [13] | Tb [13] | Dy [13] | Y [13] |
|---|---|---|---|---|---|---|---|
| $x$ | 0.65 | 0.80 | 0.89 | 0.86 | 0.78 | 0.77 | 0.82 |
| $a$/Å | 4.5599(3) | 4.5439(1) | 4.519(1) | 4.488 82(5) | 4.484 86(3) | 4.474 93(4) | 4.483 50(4) |
| $c$/Å | 9.7544(9) | 9.6414(2) | 9.532(1) | 9.3658(2) | 9.3062(2) | 9.258 52(1) | 9.300 26(5) |
| Volume/Å$^3$ | 202.75(4) | 199.065(8) | 194.6(2) | 188.715(8) | 187.185(6) | 185.402(6) | 186.952(7) |

TABLE II. Obtained parameters for superconductivity of $R\mathrm{Ni}_x\mathrm{Bi}_2$.

| Compound | $T_c$/K | $H_{c1}$/Oe[a] | Volume fraction[a] |
|---|---|---|---|
| $\mathrm{LaNi}_{0.65}\mathrm{Bi}_2$ | 4.0 | 90 | 0.01 |
| $\mathrm{CeNi}_{0.80}\mathrm{Bi}_2$ | 4.2 | 65 | 0.96 |
| $\mathrm{NdNi}_{0.89}\mathrm{Bi}_2$ | 4.1 | 55 | 0.14 |
| $\mathrm{YNi}_{0.85}\mathrm{Bi}_2$ | 4.1 | 67 | 0.17 |

[a]These were estimated from an $M$-$H$ curve at 2 K.

takes place at 4.2 K. A small hump is also observed at ~7 K, as shown in the right-hand inset. The $M$-$H$ curve at 2 K in the left-hand inset of Fig. 2(b) shows a typical profile for a type-II superconductor with a lower superconducting critical magnetic field ($H_{c1}$) of ~65 Oe. Table II summarizes $T_c$, $H_c$, and the superconducting volume fraction of four kinds of $R\mathrm{Ni}_x\mathrm{Bi}_2$ compounds. Although $T_c$ is similar for the four compounds, the volume fraction of the superconductivity phase was found to be significantly enhanced in the Ce compound.

Figure 3 shows the heat capacity of $\mathrm{CeNi}_{0.8}\mathrm{Bi}_2$ as a function of temperature. A distinct $\lambda$ peak is observed only for $\mathrm{CeNi}_{0.8}\mathrm{Bi}_2$. Application of the magnetic field suppressed the $\lambda$ peak. The Sommerfeld coefficient ($\gamma$) at 5.0 K was estimated to be 0.4 $\mathrm{J\,K^{-2}\,mol\,Ce^{-1}}$ (inset of Fig. 3), which in turn led to an observable large mass enhancement of the conducting carrier, because the $\gamma$ value is proportional to the density of states at $E_F$. Such a large mass enhancement was not seen for the La or Y systems. We thus attributed the observed $\lambda$ peak to AFM ordering of the Ce $4f$ electron spin, rather than the superconductive transition on the basis of the following reasons: (1) The peak suppression behavior by H is rather different, (2) the entropy obtained from the integration of $C_p/T$ is $\sim R\ln 2$ corresponding to a doublet ground state of the crystal

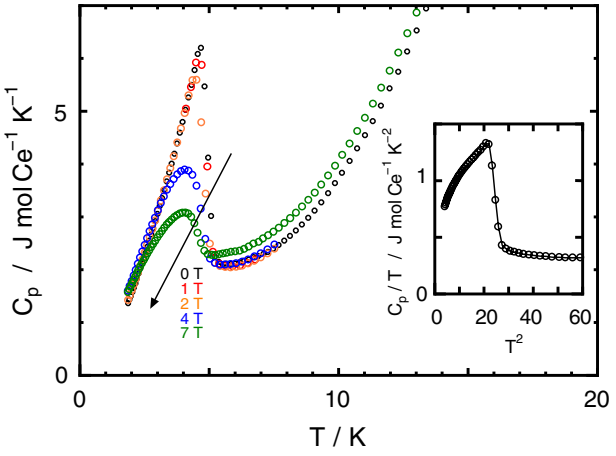


FIG. 3 (color online). Magnetic field dependence of the heat capacity of $\mathrm{CeNi}_{0.8}\mathrm{Bi}_2$ below 15 K. The inset shows the $T^2$ dependence of the heat capacity per unit temperature of $\mathrm{CeNi}_{0.8}\mathrm{Bi}_2$ at 0 Oe.

electric field of a $Ce^{3+}$ ion, and (3) if the heavy electrons give superconductive transitions, the magnitude of the $C_p$ jump should be ~2 $\mathrm{J\,mol^{-1}\,K^{-1}}$ ($\gamma T_c$); however, the observed jump was ~4 $\mathrm{J\,mol^{-1}\,K^{-1}}$. This AFM transition has also been pointed out by several groups on the basis of the magnetic susceptibility data on $\mathrm{CeNiBi}_2$ [18–20]. A similar small hump near 7 K was shown in the right-hand inset of Fig. 2(b). The evolution of the magnetic peaks for our sample was confirmed below 5 K by powder neutron diffraction [14]. The AFM ordering of the Ce $4f^1$ spin in which the magnetic moment is parallel to the $c$ axis was confirmed by the appearance of new magnetic peaks due to the disappearance of $n$-glide plane.

Mass enhancement presumably results from strong interaction of the Ce $4f$ electron with the carrier electrons, which may come from Ni $3d$ electrons mixed with Bi(1) $6p$ electrons. The peak due to superconductive transition in the specific heat was not observed. The Bi $6p$ band in the metallic Bi(2) square net contains a positive hole, which may lead to the small blocking effect against the $\mathrm{Ni}_x\mathrm{Bi}(1)$ conducting layer. The mass of carrier in the Bi(2) $6p$ band is not heavy; that is, the $\gamma$ value is smaller by an order of magnitude than the observed value of 0.4 $\mathrm{J\,K^{-2}\,mol\,Ce^{-1}}$. The $\gamma$ value for the Bi square net has not previously been reported. Thus, we estimated the $\gamma$ value from the data on similar compounds. For example, the $\gamma$ value for the $\mathrm{Ni}_{1/3}\mathrm{Bi}$ superconductor with $T_c = 4$ K is reported to be 4.3 $\mathrm{mJ\,K^{-2}\,mol^{-1}}$, and the specific heat jump $\Delta C_p$ should be $\sim\gamma T_c$, 20 $\mathrm{mJ\,K^{-1}\,mol^{-1}}$ [21]. The magnitude of this jump relative to the observed AFM peak was too small to be observed. When the light carriers coexisting with the heavy carriers cause superconductivity, the peak originating from the superconductivity is hidden by overlap of the strong peak due to the AFM transition. Therefore, the specific heat data indicated that there are two kinds of carriers with noticeably different effective masses. The heavy carrier is due to magnetic interaction between the conduction electrons and the Ce $4f$ electron which causes the AFM ordering at ~5 K, and the light carriers cause superconductivity at ~4 K. It is proposed that the origin of the light electrons comes from Bi(2) $6p$ and superconductivity occurs in the Bi square net, whereas the heavy electrons come from $\mathrm{Ni}_x\mathrm{Bi}(1)$ layers. The $T_c$ (~4 K) for $\mathrm{CeNi}_{0.8}\mathrm{Bi}_2$ is significantly higher than those of LaNiPO and Ce based mass-enhancement superconductors [3,22], although the two-dimensional electronic structure weakened by the metallic Bi blocking layer and the mass enhancement by the $Ce^{3+}$ ion should be disadvantageous for the emergence of superconductivity in the Bi(2) square net.

This work was supported by the Funding Program for World-Leading Innovative R&D on Science and Technology (FIRST), Japan. We thank Dr. S. Shamoto, Dr. K. Kodama, and Dr. S. Wakimoto (JAER) for powder neutron diffraction measurements.

*Corresponding author.
hosono@lucid.msl.titech.ac.jp

[1] Y. Kamihara, T. Watanabe, M. Hirano, and H. Hosono, J. Am. Chem. Soc. **130**, 3296 (2008).
[2] K. Ishida, Y. Nakai, and H. Hosono, J. Phys. Soc. Jpn. **78**, 062001 (2009).
[3] T. Watanabe, H. Yanagi, T. Kamiya, Y. Kamihara, H. Hiramatsu, M. Hirano, and H. Hosono, Inorg. Chem. **46**, 7719 (2007).
[4] S. Matsuishi, Y. Inoue, T. Nomura, H. Yanagi, M. Hirano, and H. Hosono, J. Am. Chem. Soc. **130**, 14 428 (2008).
[5] M. Rotter, M. Tegel, and D. Johrendt, Phys. Rev. Lett. **101**, 107006 (2008).
[6] X. C. Wang, Q. Q. Liu, Y. X. Lv, W. B. Gao, L. X. Yang, R. C. Yu, F. Y. Li, and C. Q. Jin, Solid State Commun. **148**, 538 (2008).
[7] H. Takahashi, K. Igawa, K. Arii, Y. Kamihara, M. Hirano, and H. Hosono, Nature (London) **453**, 376 (2008).
[8] G. Wang, L. Li, S. Chi, Z. Zhu, Z. Ren, Y. Li, Y. Wang, X. Lin, Y. Luo, S. Jinag, X. Xu, G. Cao, and Z. Xu, Europhys. Lett. **83**, 67 006 (2008).
[9] D. J. Singh and M.-H. Du, Phys. Rev. Lett. **100**, 237003 (2008).
[10] X. H. Chen, T. Wu, G. Wu, R. H. Liu, H. Chen, and D. F. Fang, Nature (London) **453**, 761 (2008).
[11] R. Hoffmann, *Solids and Surfaces: A Chemist's View of Bonding in Extended Structures* (VCH, New York, 1988).
[12] L. Zen and H. F. Franzen, J. Alloys Compd. **266**, 155 (1998).
[13] Y. Lu, Y. Liang, X. Yang, H. Chen, and J. Zhao, Chin. J. Struct. Chem. **24**, 769 (2005).
[14] K. Kodama, S. Wakimoto, S. Shamoto, H. Mizoguchi, and H. Hosono (to be published).
[15] W. Tromel and R. Hoffmann, J. Am. Chem. Soc. **109**, 124 (1987).
[16] TOPAS version 3, Bruker AXS, Karlsruhe, Germany, 2005.
[17] A. LeBail, H. Duroy, and J. L. Fourquet, Mater. Res. Bull. **23**, 447 (1988).
[18] H. Flandorfer, O. Sologub, C. Godart, K. Hiebl, A. Leithe-Jasper, P. Rogl, and H. Noel, Solid State Commun. **97**, 561 (1996).
[19] M. H. Jung, A. H. Lacerda, and T. Takabatake, Phys. Rev. B **65**, 132405 (2002).
[20] A. Thamizhavel, A. Galatanu, E. Yamamoto, T. Okubo, M. Yamada, K. Tabata, T. C. Kobayashi, N. Nakamura, K. Sugiyama, K. Kindo, T. Takeuchi, R. Settai, and Y. Onuki, J. Phys. Soc. Jpn. **72**, 2632 (2003).
[21] Y. Fujimori, S. Kan, B. Shinozaki, and T. Kawaguti, J. Phys. Soc. Jpn. **69**, 3017 (2000).
[22] R. Settai, T. Takeuchi, and Y. Onuki, J. Phys. Soc. Jpn. **76**, 051003 (2007).